CONFIDENTIAL. Limited circulation. For review only.

Autonomous Drone Systems for Large Structure Inspections using Lissajous Curves

Irene Grace Karot Polson, Suryadeep Nath and Debasish Ghose

***Abstract*— This paper presents a simple yet computationally less-intensive method for coverage path planning around large structures. The approach makes use of properties of Lissajous curves for the task at hand. Multiple elementary inspection surfaces and their modifications are proposed that can be used for the process of inspection. A modified drone controller with provision for data acquisition is proposed to improve the controller efficiency during the inspection. The effectiveness of our proposed approach is demonstrated through simulations in physics-based environments.**

I. Introduction

Autonomous drones and robots are widely deployed in the inspection of large structures such as bridges, buildings, ships, wind turbines, and aircraft, as it is an arduous task for the inspector to perform [1-2]. The inspection is of critical importance since missing details could affect the performance and integrity of the structure. However, as necessary as inspection is, it is also dangerous, time-consuming, and expensive as, in most cases, scaffolding is required to inspect these large structures.

The flight time of a UAV might be shorter compared to the time needed to perform a complete structural inspection of large structures; therefore, we need to use multi-drone systems to inspect these structures reliably [3-5]. Inspection missions usually involve coverage path planning, model reconstruction, and the actual inspection of the structure.

Coverage path planning (CPP) is the task of determining a path that passes over all points of an area or volume of interest while avoiding obstacles. Extensive research and development have been done for single drone path planning [6-11] and data integration to reconstruct the models [12-13] for inspection. This paper develops algorithms and methodologies for drone systems to inspect large structures such as ships or offshore oil installations.

Discrete CPP algorithms divide the planning problem into two steps: viewpoints generation to generate a discrete set of views and optimal path generation using multi-goal planning to connect the views. Continuous CPP is mainly focused on following a trajectory while perceiving sensed information continuously.

Hallermann and Morgenthal [14] have discussed visual inspection methods based on airborne photos and video taken by unmanned aerial vehicles. A GPS-based matrix system helps in flying at a constant distance to the structure. The Point of Interest (POI) feature allows flying around a structure at a constant distance to the object with a continuous orientation of the flight system and the camera towards the object's center.

The review article in [15] has put together recent work in coverage path planning and model reconstruction. Coverage path planning generates an optimized path that guarantees the complete coverage of the structure of interest to gather highly accurate shape/model reconstruction information. The drawback of the CPP solution is that they require explicit information about the structure's geometry in the form of blueprints or maps, and the optimization task is time-consuming.

The majority of existing approaches attempt to reduce the computational cost [16], that is, the time needed to compute and execute the inspection mission, avoid collision with the structure of interest, and gather information with sufficient resolution for anomaly detection. A cost-effective approach to path planning using Lissajous curves has been proposed in [17-19]. The main contributions of the research work presented in this paper can be summarised as:

1) Development of a novel 3D coverage path planning methodology using Lissajous curves.
2) Design of control system with provision for efficient data acquisition.
3) Implementation of the method for inspection of large structures through simulations in physics-based environments.

The organization of the paper is as follows, Section II defines and explores the properties of Lissajous curves that have been extensively made use of for path planning. Section III describes the controller that has been made use of in the simulations. Section IV looks at the various simulations carried out to implement the proposed strategy. Section V concludes the paper and ways to improve the usage of Lissajous curve-based coverage path planning.

II. Problem Description

The problem aims to carry out coverage path planning without the knowledge of explicit geometric features of the structure. It also focuses on reducing the high computational requirement associated with path planning. This is made possible by using Lissajous curves that only require the base radius and height of the structure.

It has two main components that are independent of each other. First is the proposed coverage path planning using just the base radius and height of the structure. The 2D Lissajous curves are then transformed to 3D and fed to the drone

Irene Grace Karot Polson is with Dept. of Aerospace Engineering, Indian Institute of Technology Kanpur, India irenegkp@iitk.ac.in

Suryadeep Nath and Debasish Ghose are with Dept. of Aerospace Engineering, Indian Institute of Science Bangalore, India suryadeepn@iisc.ac.in, dghose@iisc.ac.in

Manuscript 686 submitted to 2022 American Control Conference.
Received October 12, 2021.

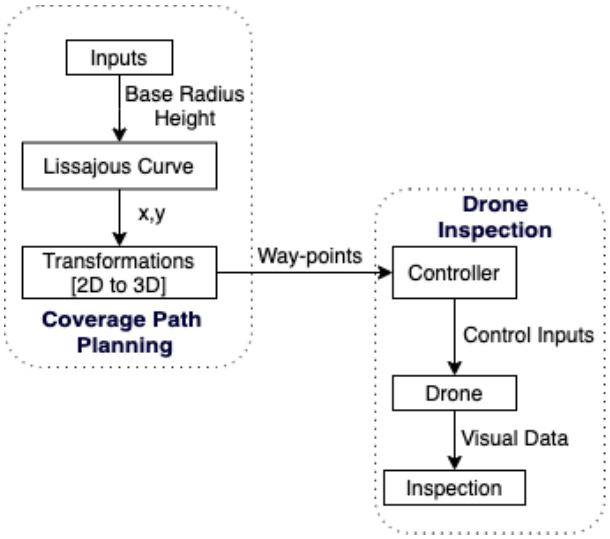

Fig. 1. Workflow of Problem Statement consisting of two tasks a) Coverage Path Planning b) Drone Inspection

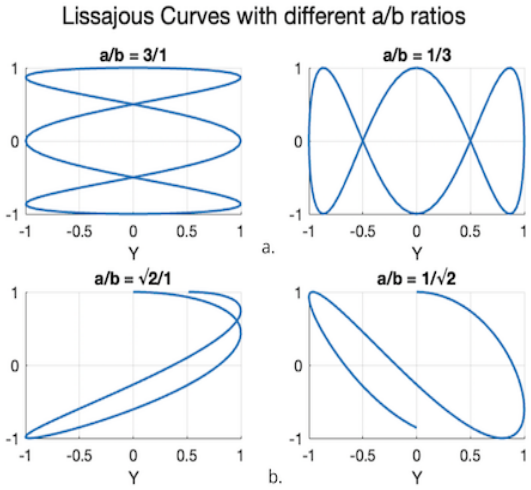

Fig. 3. a: showcases the difference in no. of lobes with a/b ratio. b: showcases curves with irrational a/b ratio.

controller as way-points. Second, the drone conducts the inspection, and data is acquired at each way-point generated by the Lissajous curves. The workflow of the strategy has been shown in the diagram in Fig.1.

III. Lissajous Curves

In this section, we look at the definition and properties of Lissajous curves that have been made use of for the problem. Lissajous figures are patterns produced by the intersection of two sinusoidal curves, the axes of which are orthogonal to each other. Such curves are chosen so that they cover an entire surface. The parametric equations that produce the curve are:

$$x = A\sin(at) \tag{1}$$

$$y = B\sin(bt + \phi) \tag{2}$$

where A and B represent amplitudes in the x and y directions and ϕ is the phase angle. Depending on the values of a and b, we can determine the number of horizontally aligned lobes and the number of vertically aligned lobes respectively.

If a/b is rational, the Lissajous curve obtained would be closed or still figures, while if a/b is an irrational, then the figure would be open and will appear to rotate with time as shown in Fig.3.

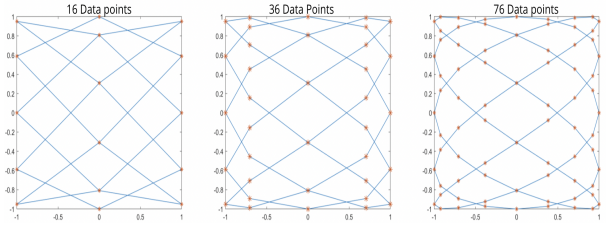

Fig. 2. Lissajous curves with different number of data-points

In our methodology, we propose to enclose the structure under consideration within a surface of revolution such as a cylinder, a cone, and variations of the same. We then make the drones trace out Lissajous curves on the surface of the revolution.

The approach is conservative, as it may not conform to the structure's shape, and the drone may move closer to certain portions of the structure than others. The method assumes that the structure is confined in the inspection surface enclosed by the Lissajous curves. However, this approach does not consider the explicit geometry of the structure to inspect, thus, saving on memory and can easily be implemented at nominal computation costs.

As Lissajous curves are on a plane, we need to describe transformations between 2D and 3D surfaces to conduct the 3D surface inspection.

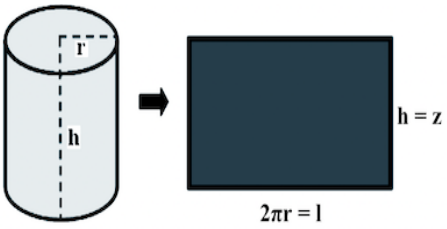

Fig. 4. Lissajous curves transformed to the surface of two separate 3-D cylinders

The Lissajous curve on the surface of a cylinder is given by

$$x = r\sin\theta \tag{3}$$

$$y = r\cos\theta \tag{4}$$

$$z = hB\sin(bt + \phi) \tag{5}$$

where r and θ are in the cylindrical co-ordinates and h corresponds to the height of the structure.

Manuscript 686 submitted to 2022 American Control Conference.
Received October 12, 2021.

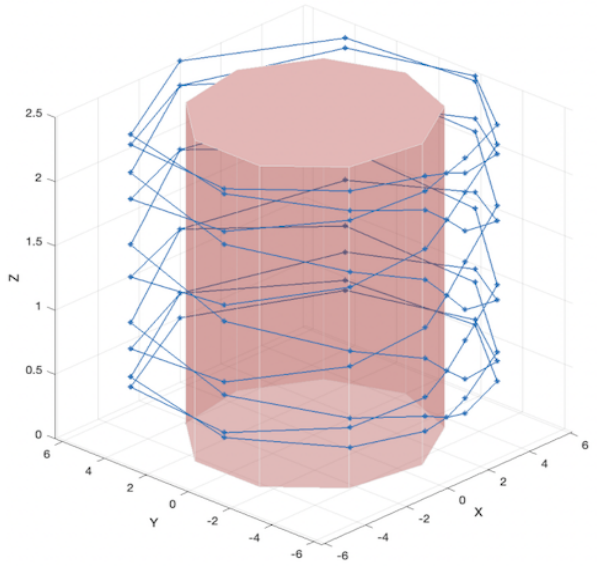

Fig. 5. Lissajous curves transformed to the surface of a single 3-D cylinder of constant radii

Let each point of the Lissajous curve be taken as a complex number represented as,

$$L = A\sin(at) + iB\sin(bt + \phi) \tag{6}$$

where real part of L is used to obtain the x and y co-ordinates while the imaginary part of L corresponds to the z co-ordinate. Let l be defined as,

$$l = A + B \tag{7}$$

The r and θ, in the cylindrical co-ordinates, corresponding to this case can be obtained as,

$$r = \frac{l \times n_1}{2\pi} \tag{8}$$

$$\theta = \frac{Re(L) \times 2\pi}{l} \tag{9}$$

and the x and y co-ordinates are obtained as,

$$x = r\sin\theta \tag{10}$$

$$y = r\cos\theta \tag{11}$$

The variable n_1 helps assign the required constant radius for the cylindrical surface covered by the Lissajous curves. The path illustrated can be carried out either completely using one drone or multiple drones.

A. Constant Radius

The most straightforward transformation carried out is the conversion from the Lissajous way-points on the plane to the surface of a single-cylinder with constant radii as shown in Fig.5.

Assuming n_1 as a constant, the radius obtained from the Lissajous curves defined would be constant, and hence the corresponding 3-D cylinder is also of constant radius. By assigning A and B as unity, we get $l = 2$ and taking n_1 as a constant C, we obtain

$$r_c = \frac{l}{2\pi} = constant \tag{12}$$

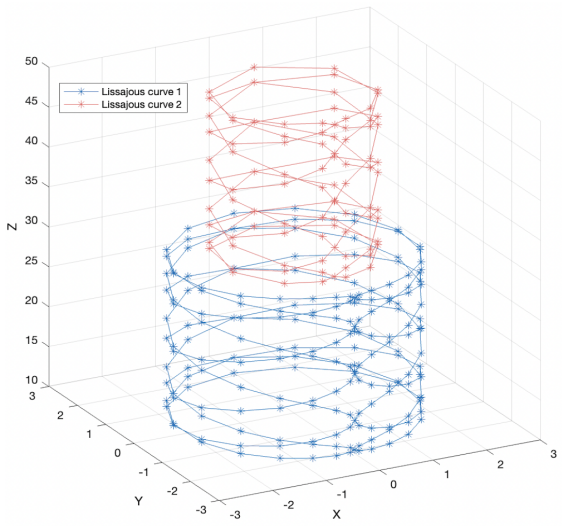

Fig. 6. Lissajous curves transformed to the surface of two separate 3-D cylinders of constant radii

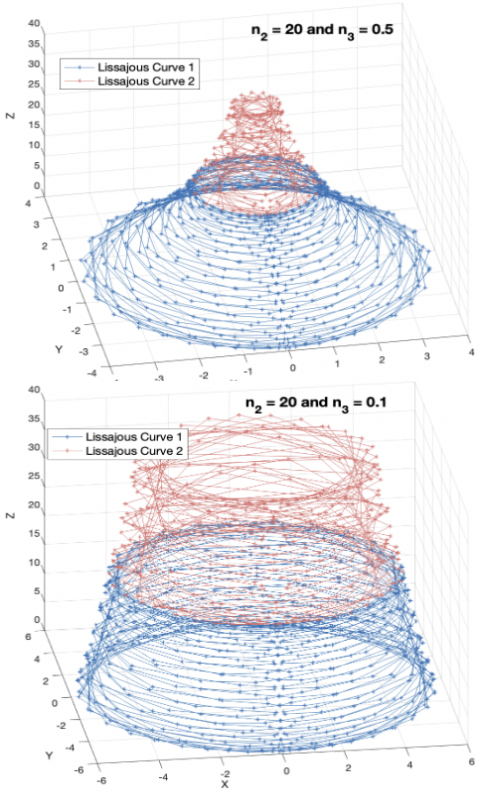

Fig. 7. The variation of n_3 that change the curvature of the inspection surface

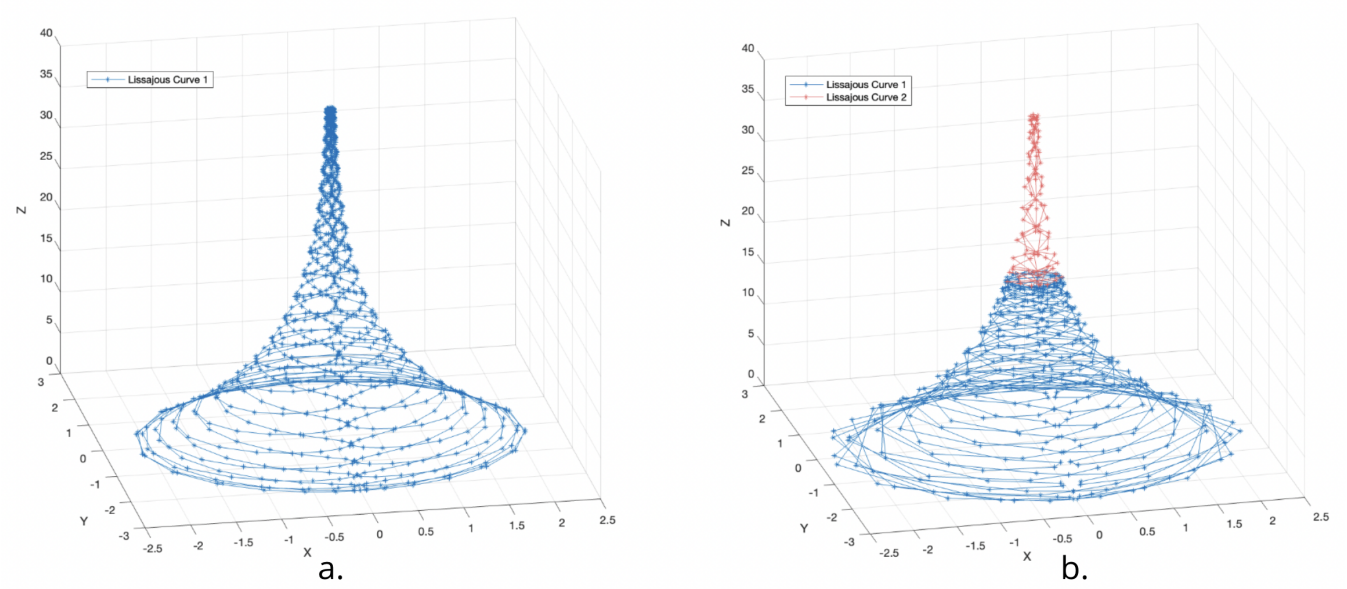

Fig. 8. a. Single Lissajous curve with continuously varying radius. b. Two separate Lissajous curves with a different number of way-point concentrations.

and the x and y co-ordinates are obtained as,

$$x = r_c \sin\theta = f_1(\theta) \tag{13}$$
$$y = r_c \cos\theta = f_2(\theta) \tag{14}$$

B. Variable Radius

The motivation behind varying the radius of the 3-D inspection surface is to facilitate the inspection of structures such as towering buildings and skyscrapers that reduce floor surface area with height. Also, having a variable radii helps in better conforming of the enclosing surface with the actual shape of the structure as shown in Fig.6.

Assuming n_1 is a function of z that is, height, such that the radius obtained from the Lissajous curves defined would be continuously decreasing, the corresponding 3-D cylindrical surface obtained would also have decreasing radii with increasing height.

By assigning A and B as unity that is, $l = 2$ and n_1 as a function of z, the choice of n_1 is made such that,

$$n_1 = \frac{n_2}{e^{n_3 \times z}} \tag{15}$$

where n_2 and n_3 are constants which decides the base radius and curvature of the inspection surface as shown in Fig.7,

$$r_v = \frac{l \times n_1}{2\pi} = f(z) \tag{16}$$

and the x and y co-ordinates are obtained as,

$$x = r_v \sin\theta = f_1(\theta, z) \tag{17}$$
$$y = r_v \cos\theta = f_2(\theta, z) \tag{18}$$

The way-points on the Lissajous curve become closely spaced with a decrease in radius, and therefore, it is necessary to adjust the number of way-points for varying radius to prevent way-point confusion for the drones and reduce redundant way-points. This is achieved by concatenating the way-points using two or more separate Lissajous curves having a different number of way-points corresponding to varying radii of the structure. Fig.8a has a single curve, while Fig.8b has two Lissajous curves: the lower one with 400 way-points and the upper Lissajous curve with 100 way-points.

IV. Controller for Inspection Drone

Drones move along the 3-D way-points generated by the Lissajous curve method, as demonstrated in Fig.5. The drones are also, additionally, required to collect data at each way-point.

The position and attitude controller developed facilitates both tracking and collection of data. For the drone in simulation, ARdrone 2.0, PD controllers were designed for position, attitude, and data acquisition.

$$e_x = X - X^* \tag{19}$$
$$e_\theta = \theta - \theta^* \tag{20}$$
$$e_{da} = P - P^* \tag{21}$$

where X, θ ,and P represent the position, attitude and pixels inside bounding box respectively and X^*, θ^* ,and P^* represent the corresponding ideal states.

The defined control laws are:

$$u_x = K_{px} e_x + K_{dx} \dot{e_x} \tag{22}$$
$$u_\theta = K_{p\theta} e_\theta + K_{d\theta} \dot{e_\theta} \tag{23}$$
$$u_{da} = K_{pp} e_{da} + K_{dp} \dot{e_{da}} \tag{24}$$

where u_x, u_θ and u_{da} are the control inputs provided to the drone. The controller gains obtained through trial and error tuning are presented in Table.1.

Manuscript 686 submitted to 2022 American Control Conference.
Received October 12, 2021.

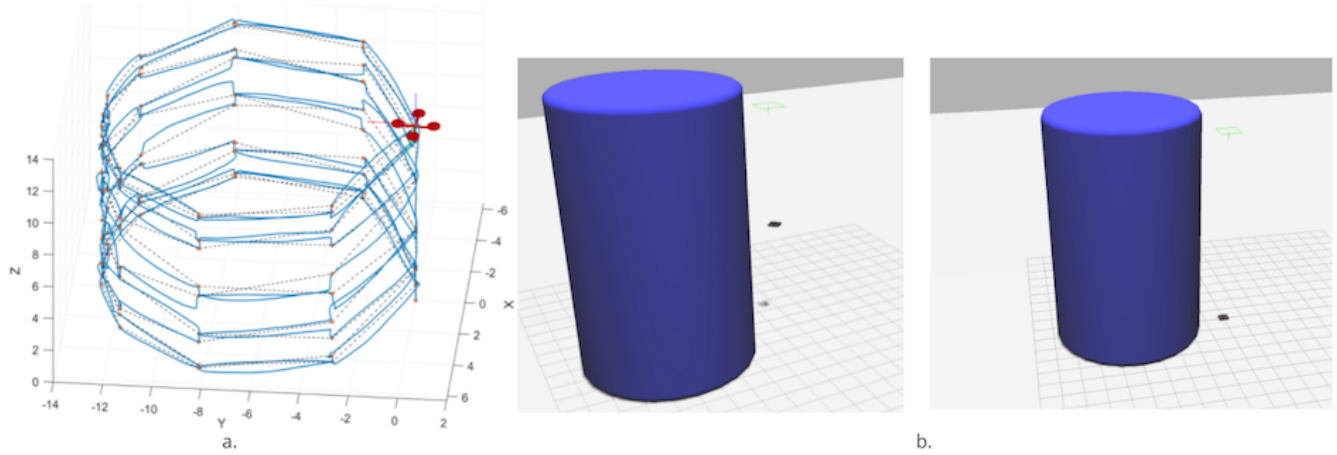

Fig. 9. a. The trajectory followed by the ARdrone 2.0 drone in 3D along the transformed cylindrical surface. b.The ARdrone 2.0 drone in 3D during simulation. `Simulation Videos`

Table 1: Controller Gains

Controller	PD gains
Position	K_{px} =2.0, K_{dx} =2 $\times 10^{-3}$
Attitude	$K_{p\theta}$ =0.4, $K_{d\theta}$ =4 $\times 10^{-3}$
Data Acquisition	K_{pp} =0.2, K_{dp} =2 $\times 10^{-3}$

Various simulations carried out in the ROS-Gazebo environment for coverage path planning with way-points generation using Lissajous curves are elucidated in the next section.

V. Simulations

Initially, a two-dimensional on-ground simulation was carried out as shown in Fig. 10. Apart from control, a provision for stopping, turning to the structure, and collecting data at each way-point was developed. The simulation was carried out using Turtlebot3, and the structure was a cube of 1m side length.

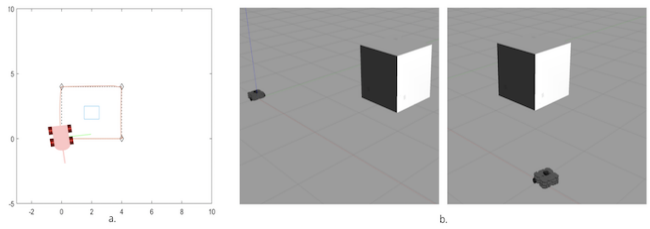

Fig. 10. (a) The trajectory followed by the turtlebot. (b) The Gazebo shots captured at the first corner during data collection.

The objective of the exercise was to facilitate the adjustment of position from structure surface-based of the number of pixels captured by the camera inside a bounding box determined around the cube structure.

Fig. 11. Images saved in the 2D path following problem at each way-point.

The data collection takes place after the number of pixels of the cube inside a generated bounding box in real-time is in the desired range. This constraint makes sure that the distance of the Turtlebot from the structure is in the desired range as well. The same depth perception concept was adopted in the 3D data gathering problem to ensure uniformity in collected images.

The 3-dimensional coverage path planning is implemented using a drone simulation. The ARdrone 2.0 that is used for simulation is controlled and made to follow the trajectory using PD controllers for both position and altitude. The trajectory the drone was made to follow are shown in Fig. 9. Throughout the data acquisition, the drone is stabilized at the altitude using a PD controller.

Table 2: Input Parameters for Path Planning

Parameters	Value
Base radius	6m
Height	10m
Number of way-points	100

The structure constructed was as a cylinder with radius $r = 6m$ and height $h = 10m$, and these are fed as the input to the proposed coverage path planning algorithm as shown in Fig.1.

The trajectory generated by the Lissajous curves can cover the surface of the entire structure, and at the same time, they can be easily split into multiple drones operations. The division is done such that the Lissajous curve time series are not disrupted, and hence it is a very convenient way to plan multi-drone paths.

It was observed during the simulation that the drone was quite faithful in following the path described by our methodology, as shown in Fig. 9, with stability and applies corrections when required. But faced difficulty navigating when the way-points were too close to each other. Hence, reducing data points on the Lissajous curves with closely spaced way-points is necessary to avoid indecision and delays in the controller. Finally, as performed in the Turtlebot simulation, the drone switches to the data acquisition

Manuscript 686 submitted to 2022 American Control Conference.
Received October 12, 2021.

Fig. 12. Images collected in simulation using MATLAB Desktop Prototyping. A total of 101 images are collected corresponding to each way-point, 8 of them are presented above.

controller at each of the way-points and adjusts itself to the capture images shown in Fig. 12.

VI. Conclusions

Through this paper, a new solution to coverage path planning is proposed and implemented for 3D structures. The use of Lissajous curves to generate way-points and trajectories gives us a relatively simple and computationally efficient process to carry inspections with complete coverage. Simulation carried out shows the feasibility of this method. The radius of the enclosing surface used to create the 3D Lissajous curves can be varied with time and height to better conform with the structure. The challenge of way-points moving closer to each other is mitigated by reducing the number of way-points with a decrease in radius. The simulations are carried out using ROS-Gazebo tum_simulator with ARdrone 2.0 and Turtlebot as the drive-robot. In the future, optimizing the path to energy or time expenditure and including multiple drones to carry out the structural inspection can be implemented to improve the current setup. The above-presented methodology can be used for cases that do not require explicit knowledge about the geometry of the structure.

References

[1] Yang, Q., Yoo, S.-J., "Optimal UAV Path Planning, Sensing Data Acquisition Over IoT Sensor Networks Using Multi-Objective Bio-Inspired Algorithms," *IEEE Access*, vol. 6, pp. 13671–13684, 2018

[2] Zhan, C., Zeng, Y., Zhang, R., "Energy-efficient data collection in UAV enabled wireless sensor network," *IEEE Wireless Communications Letters*, vol. 7, pp. 328–331, 2018.

[3] Ahmed, N., Pawase, C.J., Chang, K., "Distributed 3-D path Planning for Multi-UAVs with Full Area Surveillance Based on Particle Swarm Optimization," *Applied Science*, vol. 11, 3417, 2021.

[4] Borrelli, F., Subramanian, D., Raghunathan, "A.U. MILP and NLP techniques for centralized trajectory planning of multiple unmanned air vehicles," *American Control Conference*, p. 6, 2006

[5] Milan E., Osamah S., Enrico N., and Isabelle F., "UAVs that Fly Forever: Uninterrupted Structural Inspection through Automatic UAV Replacement," *Ad Hoc Networks*, 94, 101612, 2017

[6] Yang, K., Sukkarieh, S, "Real-time continuous curvature path planning of UAVs in cluttered environments," *5th International Symposium on Mechatronics and Its Applications*, pp. 1–6, 2008.

[7] De Filippis L., Guglieri G., Quagliotti F., "Path Planning strategies for UAVs in 3D environments," *Journal of Intelligent Robotic Systems*, vol. 65, pp. 247–264, 2012.

[8] Carsten J., Ferguson D., Stentz A., "3d field d: Improved path planning and replanning in three dimensions," *IEEE/RSJ International Conference on Intelligent Robots and Systems*, pp. 3381–3386, 2006.

[9] Masehian E., Habibi G., "Robot path planning in 3D space using binary integer programming," *World Academy of Science, Engineering and Technology*, vol 23, pp. 26–31, 2007.

[10] Chamseddine A., Zhang Y., Rabbath C.A., "Flatness-based trajectory planning/replanning for a quadrotor unmanned aerial vehicle," *IEEE Transactions on Aerospace and Electronic Systems*, vol. 48, pp. 2832–2848, 2012.

[11] Hasircioglu I., Topcuoglu H.R., Ermis M., "3-D path planning for the navigation of unmanned aerial vehicles by using evolutionary algorithms," *10th Annual Conference on Genetic and Evolutionary Computation*, pp. 1499–1506, 2008.

[12] A. Yuniarti and N. Suciati, "A Review of Deep Learning Techniques for 3D Reconstruction of 2D Images," *12th International Conference on Information Communication Technology and System (ICTS)*, pp. 327-331, 2019.

[13] L. Madračević and S. Šogorić, "3D Modeling From 2D Images," *33rd International Convention MIPRO*, pp. 1351-1356, 2010.

[14] Norman H., Guido M., "Visual inspection strategies for large bridges using Unmanned Aerial Vehicles (UAV)," *International Conference on Bridge Maintenance, Safety and Management*, 2014.

[15] Randa A., Tarek T., Lakmal S., Jorge D., Guowei C., "A survey on inspecting structures using robotic systems," *International Journal of Advanced Robotic Systems*, 2016.

[16] Englot B and Hover F., "Sampling-based coverage path planning for inspection of complex structures," *International Conference on Automated Planning and Scheduling*, pp. 29–37, 2012.

[17] Borkar, A., Sinha, A., Vachhani, L., Arya, H. (2016). Collision-free trajectory planning on Lissajous curves for repeated "Multi-agent coverage and target detection," *IEEE/RSJ International Conference on Intelligent Robots and Systems (IROS)*, 2016.

[18] Borkar, A.V., Aseem, Hangal, S., Arya, H., Sinha, A., Vachhani, L.. (2018). "Reconfigurable formations of quadrotors on Lissajous curves for surveillance applications," *Computing Research Repository*, abs/1812.04904, 2018

[19] Borkar, A.V., Sinha, A., Vachhani, L. et al. "Application of Lissajous curves in trajectory planning of multiple agents," *Autonomous Robots*, vol. 44, pp. 233–250, 2020.

Manuscript 686 submitted to 2022 American Control Conference.
Received October 12, 2021.